Supra-arcade Downflows in Long-Duration Solar Flare Events

D. E. McKenzie
Montana State University,
Bozeman, Montana 59717
U.S.A.

Abstract.
This report seeks to introduce the reader to a set of observations made during the decay phase of long duration event (LDE) flares on the Sun. In a number of events, the soft X-ray images from *Yohkoh* SXT indicate a downward directed flow field in the region immediately above the flare arcade. The prototypical event is the M5 flare of 20 January 1999, presented by McKenzie & Hudson (1999); since the time that paper was completed, eleven more events, all related to coronal mass ejections, have been found in the interval 01 January 1998 to 08 May 1999. As in the 20 January event, the speeds of downflow are 45 – 500 km s^{-1}, lower than both the freefall speed and the typically assumed Alfvén speed. A comparison is drawn between the SXT observations and the EUV and Hα data, where such are available. Important additions to our knowledge since the first paper are: (i) the motion is evidenced by both dark and bright (i.e., X-ray emitting) features, some of which may have a looplike morphology; (ii) no cool counterparts have been detected in Hα or EUV observations. The data are compared to the expected appearance according to two likely (and opposing) interpretations: an "above-the-arcade coronal rain" interpretation and a "shrinking magnetic flux tube" interpretation. In the current standard explanation of the formation of post-CME arcades, motion of the latter type may be related to outflow from a reconnection site. Movies depicting some of the flare events are on the accompanying CD-ROM.

1. Introduction

The recent report by McKenzie & Hudson (1999, hereinafter Paper I) describes motion above a solar flare long-duration event (LDE) arcade. The motion, detected in *Yohkoh* Soft X-ray Telescope (SXT) images of the flaring region, originates some 4×10^4 km above the top of the arcade and is directed downwards into the flaring region. The observations were interpreted as evidence of one of three possible scenarios: (1) dense blobs of cool material break away from the preceding coronal mass ejection and fall gravitationally back into the flaring region; (2) large-scale islands of magnetic flux form within a current sheet situated above the flare arcade; (3) flux tubes linking the current sheet, having undergone reconnection at some location high above the arcade, retract into the arcade under the force of magnetic tension. Scenarios 1 and 3 are the most easily testable with currently available data, and are the subject of the current report.

Scenario 1 is perhaps the physically simplest explanation, as it seems to require no special actions on the part of the coronal magnetic field, but only implies that some portion of the CME material fails to achieve escape velocity. There has been some speculation that such "CME backwash" material might contribute to the coronal rain which is commonly observed in post-flare Hα loops. In the current standard explanation of the formation of coronal rain, plasma which has been evaporated up into the tops of the flaring loops (Forbes & Malherbe 1986, Schmieder et al. 1987, Švestka 1989) radiates away its energy and cools through a thermal instability (Goldsmith 1971); the cooling material condenses and drains gravitationally down the legs of the post-flare loops (Foukal 1976). If CME material were observed to be falling back into the flare region, this material might be channeled (by the open field lines above the arcade) into the top of the post-flare loops, thereby contributing a possibly significant source of coronal rain material. Thus what appears to be the physically simplest explanation of the observations of Paper I would constitute an addition — but not necessarily a challenge — to the current coronal rain explanation.

As an alternative, scenario 3 is equally tempting because of its implications for the reconnection model of solar flares. As a consequence of the standard picture of the formation of post-CME arcades (the Carmichael-Sturrock-Hirayama-Kopp-Pneuman picture, see e.g. Forbes & Acton 1996 and references therein), the field lines which have been opened to space by the eruption and subsequently reconnected should retract away from the reconnection site under the force of magnetic tension. Some reports of observational evidence for this field line shrinkage have appeared (Hiei & Hundhausen 1996, Forbes & Acton 1996), though on temporal and/or spatial scales much greater than the observations of Paper I. The discussion is further fueled by the discovery by Wang et al. (1999) of cusp-shaped features in SOHO/LASCO images. The features reported by those authors are observed to move downwards towards the Sun. Wang et al. tentatively interpret these features as "signatures of the gradual closing-down of magnetic flux" and as having the appearance of "the retraction of a series of narrow looptops". The proposed interpretation is strikingly similar to scenario 3.

A key issue in understanding the flow field above the LDE arcade is identification of the tracers of the motion — are they blobs of material like coronal rain, or are they loops connected to photospheric footpoints? Both interpretations yield explanations for the darkness of the X-ray voids described in Paper I: coronal rain material is typically too cool to emit significant intensities of X-rays, while by definition the evacuated flux tubes suggested by McKenzie & Hudson (1999) have negligible emission measure. Therefore more information is required for an adequate discrimination between these two possible explanations.

A conclusive test of scenario 1 would be measurement of the temperature of the tracers of the motion. Estimates based on integrated images, by Švestka et al. (1998) and by McKenzie & Hudson (1999), have been attempted and indicate temperatures in excess of 5 million kelvins in the fan and in X-ray voids. We note, though, that due to instrumental effects like scattering and vignetting (Foley et al. 1997) it is extremely difficult to extract accurate temperatures from flare images, especially from regions with low emission.

If a moving feature contains plasma cooler than about 2 million kelvins, then its emission, while invisible to SXT, may be detectable in some longer-wavelength passband. In particular, extreme ultraviolet (EUV) and hydrogen Balmer alpha (Hα) have been used in the present study to extend the range of temperature coverage, so that blobs or loops that are not devoid of plasma may be observable. In this way, the shape of the tracer becomes a test of the explanation of the velocity field. More precisely, the observation of X-ray or EUV emitting loops retracting into the top of the arcade would lend support to scenario 3.

A further test is the speed of downward motion: gravitational acceleration would yield speeds of the tracers of the motion less than the freefall speed; i.e., less than (or possibly equal to, but never greater than) the escape speed of 600 km s^{-1}. It is frequently stated that reconnection outflow jets, created by field lines retracting from the reconnection site, should travel at the Alfvén speed, and this speed is often assumed to be on the order of 1000 km s^{-1}. However, Forbes & Acton (1996) point out that the speed of the field line shrinkage (and thus the existence of outflow jets) depends on the local magnetic field and plasma pressure, and may be significantly lower than typically assumed. Moreover, the Alfvén speed itself, given by $v_A = \sqrt{B^2/4\pi\rho}$, is not well known in the corona, because of the difficulty of measuring the magnetic field. For a plasma density $\rho = m_p \times 10^9\ cm^{-3}$, a magnetic field strength between $B = 5$ — 50 G yields $v_A = 350$ — 3500 km s^{-1}.

Furthermore, if the flow field reported in Paper I is due to the outflow or shrinkage of field lines away from a reconnection site, then the appearance is contrary to the smooth and continuous outflow expected from 2-D and 2.5-D simulations. The apparent retractions of *individual* reconnected flux tubes is more reminiscent of the "patchy and intermittent" reconnection which Klimchuk (1997) describes as a product of a true 3-D configuration. Confirmation of scenario 3 would thus have ramifications for models of magnetic reconnection in solar flares.

Pursuant to these motivations, a search of the SXT data archive was undertaken to find more examples of supra-arcade downflow in LDE flares. When flows were located, the data catalogs of SOHO/EIT, TRACE, and MLSO Hα were consulted to find contemporaneous data. This study, the first multi-instrument search for supra-arcade downflows, was primarily designed to look for cooler counterparts to the X-ray voids. Any observations of X-ray *emitting* features undergoing shrinkage would be considered serendipitous.

Yohkoh SXT is a broadband instrument with sensitivity to plasmas with temperatures between approximately 1 – 50 million kelvins (Tsuneta et al. 1991). The 195 Å and 171 Å passbands of SOHO/EIT and TRACE have peak responses to plasmas near 1.5 and 1 million kelvins, respectively (Delaboudiniere et al. 1995, Moses et al. 1997, Handy et al. 1999, Schrijver et al. 1999). Hydrogen-alpha emission is typically formed around 10 thousand kelvins. It was felt that the combination of SXT, 195 Å , 171 Å , and Hα (where available) would provide an adequate range of temperature sensitivity to detect blobs of cool material falling gravitationally into an arcade, despite the significant gap in coverage between the temperatures of line formation represented by these passbands. Data gathered by this combinatory approach would provide evidence for one or the other scenario: blobs visible in cooler passbands corresponding to the X-ray voids, or hot shrinking loops. The former might appear in any of the selected passbands, if the blobs are warm enough to emit radiation. Since the reconnected loops are imagined to pass through slow shocks and thereby be heated before retracting into the arcade (Cargill & Priest 1983, Forbes & Malherbe 1986, Forbes & Acton 1996), the latter probably would only be visible in SXR or EUV emission.

The detection of absorbing material, or of true voids (e.g., *evacuated* flux tubes), is much more problematic, as a bright background is required to see the dark features in contrast. In the SXT observations this bright background is provided by the supra-arcade fan (see Figures 1, 3); but the fan is invisible in the EUV and Hα images (except in a few of the 195 Å images, where the fan is just faintly discernible). In events where the LDE arcade projects above the solar limb, the absence of a readily detectable arcade fan renders any non-emitting supra-arcade features (blobs, loops, anything) invisible against the background of dark space. For events on the solar disk, the situation is not so hopeless; but detection of absorbing features with sizes on the order of 10^9 cm is extremely challenging, given the faintness of contrast expected (based on comparison to the contrast in the SXT images) and the speed at which the features are observed to move.

The data archive search revealed an additional 11 supra-arcade downflow events; all have evidence of downward moving X-ray voids. In what follows, we present a description of the 12 downflow events within the search period, characterizing downflow velocities where measured (i.e., by feature tracking in the SXT images), and the appearance in EUV and Hα images, where such data are available. In section 2 we describe the general characteristics of the archive search and of the data, after which we summarize the details of the observations on a case-by-case basis in section 3. Section 4 comprises a discussion and interpretation of our findings; conclusions are in section 5. Movies depicting some of the flare events are on the accompanying CD-ROM; captions for these movies are included in the Appendix to this report.

2. Data Archive Search: General Considerations

This section comprises a description of the criteria used in the archival data search, the preparation of the data, and the capabilities of each data set.

2.1. Soft X-rays

Following the discovery reported in Paper I, we embarked upon a search of the archival SXT data in an effort to ascertain whether the downward flows are a common occurrence. The search was restricted to flares of GOES M1.0 and larger, during the period between 01 January 1998 and 08 May 1999, inclusive. These limitations are not entirely arbitrary, but were chosen to allow a large yet manageable number of flares to be examined. The SXT archives contain data for 118 solar flares satisfying these criteria. The soft X-ray (SXR) images of these flaring structures were visually analyzed; arcade fans were observed in 22 events, and supra-arcade downflows were detected in 12 of those. The dates and times of these 12 events are given in Table 1, with the GOES classification of the X-ray flare associated with each.

The SXT images most appropriate for viewing the supra-arcade downflows were determined to be the half-resolution (4.9 arcsec/pixel) partial-frame images made during SXT's automatically triggered flare mode. Since at least late 1997 these have been acquired in the AlMg and Al12 analysis filters (Tsuneta et al. 1991) at a cadence of approximately one AlMg+Al12 pair per 18 – 20 seconds during high-bitrate sequences, and one pair per 128 seconds at medium bitrate. Two important considerations, aside from the spatial and temporal resolution of these

Table I. List of twelve supra-arcade downflow events. X-ray flare classifications and start- and peak-times are from GOES, as reported by the NOAA Space Environment Center. A "late" entry in the last column means that Hα data were acquired, but some hours after the flows were observed in SXT. All these events were associated with coronal mass ejections.

Date	GOES Start, Peak (UT)	SXT flow time (UT)	GOES classification	EUV exist?	Hα exist?
20 Apr 1998	09:10, 10:21	09:43 - 16:42	M1.4	Y	N
23 Apr 1998	05:35, 05:55	06:55 - 07:12	X1.2	Y	N
27 Apr 1998	08:55, 09:20	09:38 - 10:36	X1.0	Y	N
09 May 1998	03:04, 03:40	04:59 - 05:45	M7.7	Y	N
16 Aug 1998	17:37, 18:21	18:27 - 19:14	M3.1	N	Y
18 Aug 1998	22:10, 22:19	23:50 - 00:26	X4.9	N	N
30 Sep 1998	13:08, 13:50	13:32 - 14:07	M2.8	Y	late
23 Nov 1998	10:59, 11:21	11:52 - 12:34	M3.1	Y	N
18 Dec 1998	17:13, 17:22	18:18 - 18:23	M8.0	N	Y
20 Jan 1999	19:06, 20:04	20:36 - 21:32	M5.2	N	Y
03 May 1999	05:36, 06:02	06:04 - 07:08	M4.4	Y	N
08 May 1999	14:22, 14:40	14:33 - 14:52	M4.6	Y	late

images, are the field of view and the exposure duration. The field of view of these images is 5.2 × 5.2 arcmin, wide enough to include the bright arcade and a large fraction of the supra-arcade fan. The exposure duration of the half-resolution images is ordinarily held fixed (248 msec for AlMg, 948 msec for Al12, with variation of less than 1%) during flare observations; these relatively deep exposures, while saturating the pixels centered on the bright flare arcade, enable detection of the much fainter fan (see Figures 1 & 3). In contrast, the full-resolution images (2.45 arcsec/pixel) have a field of view of only 2.6 × 2.6 arcmin, centered on the brightest part of the arcade and usually only large enough to show just that. The exposures are controlled by onboard software, intended to optimize the image quality (i.e., no saturation or underexposure); the result is optimal exposures for the brightest part of the arcade but no detection of the fan. Conversely, the quarter-resolution images which are also made with fixed exposure duration during a flare have too coarse of spatial resolution to clearly show the motion of the arcade. The X-ray voids described in Paper I are typically only 1 – 3 half-resolution pixels wide, or 0.5 – 1.5 quarter-resolution pixels. Examples of SXT image sequences showing the supra-arcade downflows, to be discussed in more detail below, are Enclosures 1, 2, and 3 on the accompanying CD-ROM. The preparation of the images included decompression, exposure normalization, subtraction of dark current and known stray light, and co-alignment.

The SXT images facilitate measurement of the speed and size of the tracers of the motion. In most cases these tracers are the X-ray voids discussed in Paper I; the signal in these regions is too low and too near the bright arcades (which are a source of scattered photons) to allow meaningful measurement of temperatures. For the reasons stated in section 1, plus the double-valued nature of the Al12/AlMg ratio (Tsuneta et al. 1991), no temperature measurements of the X-ray voids will be attempted in the present report.

2.2. Extreme Ultraviolet

The Extreme-ultraviolet Imaging Telescope (EIT) on board SOHO (Delaboudiniere et al. 1995, Moses et al. 1997) and the Transition Region and Coronal Explorer (TRACE: Handy et al. 1999, Schrijver et al. 1999) are both normal-incidence telescopes that make use of multilayer mirror coatings to focus EUV radiation in more than one wavelength passband; the passbands most used in the current study are the 195 Å of EIT and the 195 Å and 171 Å of TRACE. EIT has a full-Sun field of view and spatial resolution of 2.6 arcsec/pixel; the field of view of TRACE is 8.5 arcmin square, with spatial resolution of 0.5 arcsec/pixel.

The SOHO/EIT and TRACE data catalogs were searched for the dates listed in Table 1, for times surrounding the periods when SXR flows were observed. Images were found in the EIT archives for 7 of the events. The cadence of the observations varies from event to event, from 7 minutes to 12 minutes per image. The image preparation included exposure-duration normalization, subtraction of dark current and readout noise, degridding, and flat fielding (J. Newmark, private communication). The data were viewed both with logarithmic scaling (i.e., $image = log_{10}(data)$), and with differencing ($image = data(t_2) - data(t_1)$). In each case where EIT images were available, the flare arcade was identified and the region above the arcade, corresponding to the observed (in SXR), location of downflows, was visually analyzed (see example in Figure 1).

The cadence and spatial resolution of TRACE are generally better than EIT, but the field of view is restricted. Thus it happens that TRACE was often not looking at these regions at times coincident with the SXT observations. The TRACE archives were searched, and hold data only for the events of 30 September 1998 and 08 May 1999.

Slower cadence than SXT means motion would be visible as discontinuous apparent changes in the morphology or location of features, but said motion would be difficult to quantify precisely. The presence of

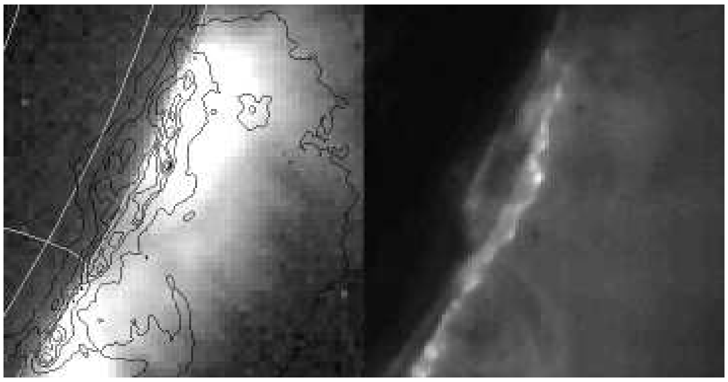

Figure 1. Comparison of SXT and EIT for 20 April 1998. The lefthand frame shows the extent of the SXT arcade at 10:58:51 UT, with the EIT arcade (from 11:02:38 UT) overlaid as contours. The righthand frame shows the appearance of the same EIT image. This is approximately one hour after the downflows were first observed in the SXT images.

blobs would be detectable, as the richness of temporal coverage is still sufficient and the exposures short enough to capture features/blobs in place.

2.3. Hydrogen Balmer Alpha

Full-Sun hydrogen-alpha (Hα) images were provided by Mauna Loa Solar Observatory for five events. The spatial resolution of the Polarimeter for Inner Coronal Studies (PICS) images is 2.9 arcsec/pixel; cadence was one image per 3 minutes. The current study utilized both full-disk and coronagraphic images. Image preparation included location of Sun center and rotation to correct for P-angle. For each of the events, a large field of view centered on the flare arcade was monitored visually, the contrast enhanced to emphasize faint features. An example Hα movie is provided in Enclosure 4 on the accompanying CD-ROM. It is unlikely that absorption would have been detected, because, as with most of the EUV, no fan is visible above the arcade. Primarily with the Hα we were looking for evidence of above-the-arcade coronal rain (scenario 1). For three of the events (16 August 1998, 20 January 1999, and 18 December 1998) the Hα data are contemporaneous with the SXT downflows (i.e., during the time when SXT actually sees X-ray voids). For the other two events (30 September 1998, 08 May 1999) Hα images were made several hours after the observations of X-ray voids. Although no SXR downflows were observed at these later times, analysis of these “late” Hα data is justified by the observation in Paper I of downflows up to 17 hours after initiation of the flare.

3. Observations, Case by Case

In this section we summarize the observations of the 12 events on a case-by-case basis. Where possible, we compare the observations from the different passbands (SXR, EUV, Hα). Descriptions are given of the morphologies and motions seen in each event, the timing of same, and the downflow speeds in cases where they were measured. Three of the events are depicted in movies on the accompanying CD-ROM.

3.1. 20 April 1998

This M1.4 flare was associated with a large CME on the southwest limb. An erupting prominence was observed by EIT beginning at about 09:10 UT; peak SXR flux occurred at 10:21 UT. The EIT 195 Å images show the arcade billowing outwards, expanding; also they faintly reveal the arcade fan, but nowhere near as bright as it is seen in SXT. The images do not reveal downward motion or field line shrinkage.

SXT images show supra-arcade downflow between 09:43 – 16:42 UT. The speeds of 7 X-ray voids were measured: 45 – 130 km s^{-1}, at heights of 1.8 – 2.7 $\times$ 10^5 km (note that these are plane-of-sky speeds, uncorrected for projection effects).

Images from SXT (10:58:51 UT) and EIT (11:02:38 UT) are compared in Figure 1. Note that this is approximately one hour after downflows were first observed in SXT, and while the EIT arcade is still quite small.

3.2. 23 April 1998

According to the SOHO/LASCO online CME report, this X1.2 flare was associated with a partial halo CME; the flare site was approximately heliographic South 15 degrees on the east limb. Data from the NOAA Space Environment Center indicate that the X-ray flare began at 05:35 UT and peaked at 05:55 UT. SXT and EIT images show the rise phase of the flare, with long curved loops expanding outwards, and also portions of the decay phase. The SXT images clearly show X-ray voids from 06:55 – 07:12 UT; the paths of the voids are not purely radial, indicating that the motion is not purely gravitational. An SXT movie of this event is Enclosure 1 on the accompanying CD-ROM. Speeds of 5 X-ray voids were measured: 200 – 400 km s^{-1} in the plane of the sky, at heights of 3.5 – 7.0 $\times$ 10^4 km. There are five EIT 195 Å images between 06:51 – 07:19 UT; a northward-extending plume is observed, but no downward motion nor blobs above the arcade.

3.3. 27 April 1998

The halo CME and related X1.0 flare arose from approximate heliographic coordinates South 16 degrees, East 50 degrees, beginning at 08:55 UT; soft X-ray flux peaked at 09:20 UT. SXT detected supra-arcade downflow between 09:38 – 10:36 UT, though the visibility of the X-ray voids is poorer than in some other events. The 195 Å images from EIT (cadence of about one image per 15 minutes) show a Moreton-type wave at the time of the flare; also, difference images give the appearance of three "wavefronts" of coronal dimming to the north of the arcade *before* the brightening of the arcade. There is also coronal dimming in the south at the time of the arcade brightening. The EIT images suggest the outward ejection of a small amount of material at 08:51 UT, but no blobs or voids above the arcade after the formation of the arcade.

3.4. 09 May 1998

The M7.7 flare on the southwest limb (approximately heliographic South 15) began at 03:04 UT and peaked (in X-rays) at 03:40 UT. Supra-arcade downflows were observed by SXT between 04:59 – 05:45 UT, primarily in the north end of the arcade. The motions are distinctly non-radial, being inclined towards the ecliptic.

There are 12 EIT images from 03:01 – 05:48 UT, in 195 Å. From 03:44 onward, the EIT images show the small arcade and a faint northward extension which is inclined to the ecliptic, similar to the SXT fan. No blobs are caught in the images, and the cadence is too low to discern motion clearly. But the images apparently confirm that the fan is visible in 195 Å, albeit just barely.

3.5. 16 August 1998

The CME and M3.1 flare occurred on the northeast limb (heliographic North 32 degrees), beginning at 17:37 UT, the X-ray flux peaking at 18:21 UT. In addition to the approximately radial downward motion of X-ray voids between 18:27 – 19:14 UT, SXT observed the downward motion of hot, X-ray emitting plasma into the flare site. A movie of this event is Enclosure 2 on the accompanying CD-ROM; the hot shrinkage is best observed above the north end of the arcade. Hα images from 18:20 – 19:20 UT were analyzed: they show the arcade of post-flare loops but nothing above. When the Hα images are overlaid onto the SXT images, they show that the SXR arcade extends far above anything seen in Hα. Careful scrutiny of contrast-enhanced and logarithmically scaled Hα images shows nothing above the SXR arcade, particularly in the downflow region.

3.6. 18 August 1998

The X4.9 flare at the northeast limb (approximate heliographic North 33 degrees, East 87 degrees) was accompanied by a large ejection of X-ray-emitting material (cf. Ohyama & Shibata 1997, 1998, and Nitta & Akiyama 1999). The flare began at about 22:10 UT, and peaked at 22:19 UT. Downward-moving X-ray voids were observed above the southern end of the arcade between 23:50 – 00:26 UT. Unfortunately no EUV or Hα data were available.

3.7. 30 September 1998

At 13:08 UT the flare began at heliographic North 26 on the west limb, reaching peak SXR flux of M2.8 at 13:50 UT. SXT detected flows between 13:32 – 14:07 UT. Also, in the interval 13:33 – 13:40 a stream of hot material is observed being ejected from the north end of the arcade. The arcade fan is not fully developed at this time, so visibility of the X-ray voids is poor, disallowing meaningful speed measurements. However, there is some indication of shrinkage of hot (X-ray emitting) features. They appear as short, roughly linear features similar to the rays of the arcade fan; in some instances they resemble cusped looptops. After appearing above the top of the arcade they subsequently retract into it. This feature is similarly observed in a few of the other events discussed in the present paper; the 30 September 1998 and 20 January 1999 observations provide especially clear examples. A movie of the latter is Enclosure 5 on the accompanying CD-ROM.

TRACE images from 14:20 – 14:30 UT (171 Å, 1216 Å, 1550 Å, 1600 Å, 10 images each) are from the period after the SXT flow observations. These images show coronal rain material draining down the legs of the arcade. The first few images in each passband show the partial eruption of a filament in the foreground, towards the south end of the field of view; this is believed to be a separate event. No downflow is detected above the M2.8 arcade in the TRACE images.

MLSO Hα images cover the period from 17:10 – 22:24 UT. Examination of the interval 17:10 – 18:28 UT shows the classical type of coronal rain draining down the arcade legs. Nothing is observed above the arcade, even in logarithmically scaled data. This is well after the SXT downflow observations, but while there is visible drainage in Hα. Overlay images suggest that some Hα loops seem to be close to many of the contemporaneous SXR loop structures, but do not extend above the SXR features.

3.8. 23 November 1998

The location of this M3.1 flare is heliographic South 23, East 58, and the start- and peak-times listed by SEC are 10:59 and 11:21 UT. SXT detected supra-arcade downflows above the region between 11:52 – 12:34 UT; the images show exceptionally violent motion in the fan rays, and a few very clearly observed X-ray voids. Speeds were measured for 2 X-ray voids: 140 and 300 km s^{-1}, between 11:52 – 11:55 UT. Since this event is further from the limb than most, one should infer a considerable projection effect inherent in these speeds.

EIT provides a good cadence of observations: 20 195 Å images between 11:05 – 13:56 UT. The arcade is shown very clearly: bright loops expand very slowly, particularly later in the sequence. The arcade fan is detected quite faintly, but the images do not reveal bright downflowing blobs. Neither do they reveal field line shrinkage in the flare decay phase that would correspond to scenario 3 of Paper I.

3.9. 18 December 1998

Like the 23 November 1998 event, this M8.0 flare occurred at a location far onto the solar disk (heliographic North 29, East 33), so that the arcade is seen somewhat from above. Consequently the visibility of the supra-arcade downflows is not as clear as for some other events. The flare began at 17:13 UT and peaked at 17:22 UT; SXT sees downflow only during the short interval 18:18 – 18:23 UT.

Hα data from 18:03 – 18:57 were analyzed, with linear brightness scaling and also logarithmic scaling to emphasize faint features. The classic two-ribbon signature is readily apparent, but no blobs were found.

3.10. 20 January 1999

This M5.2 flare was described in Paper I; the soft X-ray flux begins increasing at 19:06 UT and peaks at 20:04 UT, at heliographic North 29 degrees on the east limb. SXT movies show clear downflowing X-ray voids between 20:36 – 21:32 UT, but some less clear examples can be found up to 17 hours after the flare onset. Movies of the SXT images from 20:36 – 20:45 UT, and the Hα images from an overlapping interval, are presented in Enclosures 3 & 4 on the accompanying CD-ROM. The speeds of 5 X-ray voids were measured: 90 – 500 km s^{-1}, at heights of 1.2 – 1.6 $\times$ 10^5 km. There is a suggestion of anti-correlation between the measured speed and the height at which the speed is measured, although this trend (which also is suggested in the measurements for 20 April 1998) is neither clear nor robust. In fact, the void measured

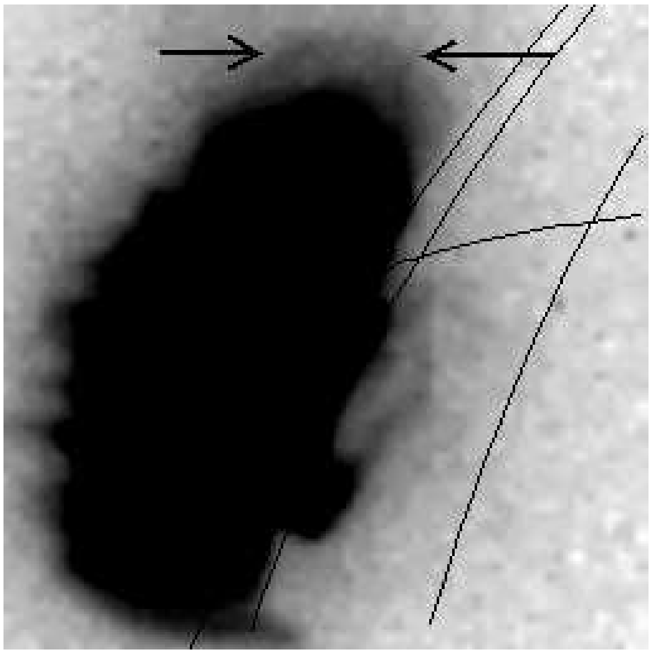

Figure 2. Contrast-enhanced image from 20 January 1999, 19:22:55 UT. In the north end of this arcade, a loop (indicated by arrows) is observed to shrink into the arcade with a plane-of-sky speed of approximately 100 km s^{-1}. See the movie in Enclosure 5.

at 500 km s^{-1} between 20:40:59 – 20:41:35 actually appears to slow to 160 km s^{-1} between 20:41:35 – 20:43:45.

Enclosure 5 on the accompanying CD-ROM shows the SXT images from 19:18 – 19:26 UT, in which one can see bright cusps which appear just above the top of the arcade, subsequently shrinking into the arcade. It is thought possible that these represent the cusped tops of recently reconnected flux tubes. This phenomenon was noticed in a few of the other events, always in the later part of the rise phase and before the formation of the tall arcade fan. Additionally, some more clearly defined X-ray emitting loops in the north end of the arcade appear to exhibit shrinkage; the apparent plane-of-sky speed is 100 km s^{-1}. (Note that the movie in Enclosure 5 will loop backwards and forwards to emphasize the motion.) An annotated and contrast-enhanced image of these loops appears in Figure 2.

Fifty-one Hα images between 19:03 – 21:36 UT were examined. They reveal post-flare loops and classical coronal rain drainage in the legs; nothing is observed in the region above the arcade. The Hα image from 20:57:26 was overlaid onto the SXT image from 20:57:53, and is shown

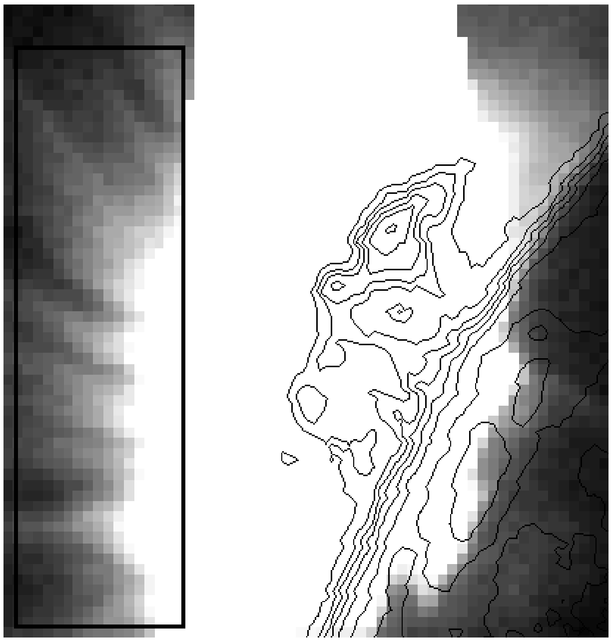

Figure 3. Overlay of Hα loops onto SXR arcade, 20 January 1999. The MLSO Hα image from 20:57:26 UT is overlaid as contours onto the SXT image from 20:57:53 UT. The region where SXT observes supra-arcade downflows is indicated by the box at left.

in Figure 3. This is a time when two X-ray voids are just reaching the base of the arcade fan. The alignment of the overlaid images appears to be fairly good (within 5 – 10 arcseconds); the Hα loops are clearly beneath the SXR arcade, primarily existing in the northern half of the arcade.

3.11. 03 May 1999

LASCO reported a halo CME from this M4.4 flare, which occurred at heliographic North 15, East 32 degrees. Soft X-ray flux began increasing at 05:36 UT and peaked at 06:02 UT; SXT very clearly observed downflows between 06:04 – 07:08 UT. The speeds of 7 X-ray voids were measured: 180 – 300 km s^{-1} in the plane of the sky. An attempt was made to correct these plane-of-sky speeds for projection effects, assuming the motion was purely radial: the resultant speeds are between 260 – 420 km s^{-1}.

EIT produced 13 images in 195 Å between 05:00 – 07:48 UT. The arcade fan is faintly visible, and some stubby rays, between 06:00 – 06:36 UT. The cadence is very slow, but no blobs were detected.

3.12. 08 May 1999

This M4.6 flare occurred near the northwest limb (heliographic North 23, West 75 degrees) and was associated with a fast, large, and bright CME observed by LASCO. Flare onset was at 14:22 UT, and the peak SXR flux was at 14:40 UT. Supra-arcade downflows were observed by SXT during the short interval 14:33 – 14:52 UT. The visibility of the small X-ray voids is not as clear as in some other cases. The voids can be seen along the whole length of the top of the arcade, at the base of the stubby arcade fan.

EIT produced 10 images in the 195 Å passband between 14:00 – 15:48 UT. The images show an interesting amount of activity in the region, beneath the flare arcade. A traveling brightening is observed propagating along the top of the arcade, from south to north. There is, however, no evidence of activity above the arcade, even in the contrast-enhanced data.

TRACE produced images in the 171 Å, 284 Å (1.2 – 4 million K), and 1600 Å (4 – 10 thousand K) passbands, between 14:25 – 15:16 UT. These images show loops and ejecta above the flare site, but nothing moving downward. In the 171 Å images emitting and absorbing loops are visible, but the arcade fan is not. A single tall plume is seen stretching upwards; this faint structure appears to be expanding outwards slowly, in approximately the same location as the downflow observed by SXT.

MLSO produced Hα images between 17:35 – 22:38 UT, which is some time after the SXT downflow observations. The images show coronal rain of the classic type. The Hα images were overlaid onto the SXT images, and it can be seen that the Hα loops are low compared to the SXR arcade. The highest-hanging Hα material is at a location comparable to the top of the arcade or the base of the SXR fan, but as before no blobs are seen in Hα above the loops.

4. Discussion

The SXT images show many examples of X-ray voids in downward motion, and a few examples of X-ray-bright features apparently shrinking. The downflow is observed in the decay phase of all these 12 flares, and in the late part of the rise phase in a few of the flares. Some of the X-ray-bright shrinking features do appear vaguely looplike, particularly (a) the 2 shrinking features in the north end of the 16 August 1998 arcade, (b) the cusplike features just above the top of the 20 January 1999 arcade, and (c) the well defined loop in the north end of the 20

January 1999 arcade. A contrast-enhanced and annotated image of (c) is shown in Figure 2. The apparent speed of this loop is estimated at 100 km s^{-1} in the plane of the sky.

The speeds measured from the SXT images are all below the escape speed of 600 km s^{-1}, and so are consistent with a purely gravitational explanation. This may be seen from a consideration of Newtonian physics: the fastest X-ray void speed from the 20 January 1999 event was measured as 500 km s^{-1} at about 20:41:17 UT. To achieve this speed under constant gravitational acceleration, a blob would have to accelerate over a distance of 460 Mm, starting from rest at about 20:10:36 UT. Given that the speed of this X-ray void was measured at a location 142 Mm above the photosphere, and assuming that the CME was launched no later than 19:00 UT, then the purely gravitational explanation is consistent with the measured X-ray void speed as long as the CME rises at a speed not less than $\approx$ 140 km s^{-1}. The same analysis applied to the X-ray void speeds of the 23 April 1998 event requires a CME rise-speed of at least 240 km s^{-1}. These requirements are below the speeds of known CME-related X-ray ejecta (Ohyama & Shibata 1997, 1998; Nitta & Akiyama 1999).

However, the detected speeds are also consistent with (or greater than) magnetic field line shrinkage speeds reported by Hiei & Hundhausen (1996), and Forbes & Acton (1996). Forbes & Acton point out that while the force driving the motion is magnetic tension, the plasma pressure will limit the maximum achievable speed. Thus although speeds incongruent with scenario 1 were not detected, neither were velocities measured which refute scenario 3.

The reader is also reminded that these are nearly all plane-of-sky speeds, uncorrected for projection effects. The true speeds are necessarily higher, but without knowledge of the true direction of motion (i.e., the departure from radial, or the component along the line of sight) we cannot make a precise guess of the correction required. However, most of these events are near the solar limb and the arcades oriented nearly perpendicular to the line of sight. It is therefore unlikely that the velocity component along the line of sight is any greater than $\approx$25% of the plane-of-sky component. Thus the difference between these plane-of-sky speeds and the true speeds is probably small.

There is also some possibility that an observational selection effect may have prevented the detection of faster motions. In an interval of 54 seconds (4 images at 18 seconds cadence), a 700 km s^{-1} feature would traverse $\approx$38 Mm, or 11 SXT half-resolution pixels. This range is just at the limit of visibility of several of the arcade fans (and beyond the range of visibility of some), which quickly become fainter with height.

Therefore it is possible that faster image cadences and deeper exposures will reveal faster downflows.

In general the EUV images beautifully display the arcades, with very thin, well defined loops. These loops exhibit expansion, and violent "waving" motions. However, there is no evidence of downflow or of blobs above the arcades. The cadence is an order of magnitude slower than SXT; poor cadence will affect the detection of motion, but will not completely explain the non-detection of macroscopic objects like blobs. The fact that the arcade fan was faintly visible in a few of the 195 Å images, but not in 171 Å, suggests the possibility of temperatures in excess of 10 million kelvins: the 195 Å passband includes a contribution from Fe XXIV (J. Gurman, private communication), with characteristic temperature of about 12 MK. The 171 Å channel of TRACE does not have this extra-hot constituent, but has significant overlap with the 195 Å channel for lower temperatures. For comparison, Švestka et al. (1998) found temperatures with SXT of 5 – 8 MK for an arcade fan of 29 August 1992; McKenzie & Hudson (1999) estimated 8 MK for the arcade fan of 20 January 1999.

As with the EUV, the Hα images show arcade loops, cooler and lower than the SXR loops. Figure 3 demonstrates the disparity in locations of the Hα material and the X-ray supra-arcade downflows. In the cases examined the SXR loops are $1.8 - 3.5 \times 10^4$ km above the contemporaneous Hα loops. This is consistent with the commonly observed relationship of flare arcades and post-flare loops (Švestka 1987). The cadence of Hα images provided by MLSO is better than the cadence of EUV images used in the present study, and should be sufficient to permit the detection of cool blobs. To test this, the cadence of an SXT image sequence was degraded to one image per 3 minutes to mimic the conditions of the Hα observations. Violent motions were clearly observed in the rays of the arcade fan, just as is visible in some of the EUV movies. As expected, this slower cadence is insufficient to allow the tracking of individual blobs, but the visible deformation and displacement of the fan rays indicates the presence of the flow field. It should be concluded that if blobs were in the area and were emitting in one of the passbands used in this study, they ought to have been detectable. However, the Hα images, even with extreme contrast enhancement and logarithmic scaling, do not reveal any cool counterparts to the downflow detected in the SXT images. The Hα images depict clear examples of coronal rain of the classic type, but no evidence is found that this material flows back from the CME: above the post-flare loops the Hα images show only clear empty sky.

The data suggest that there were no cool blobs, but unfortunately the available EUV images are of insufficient cadence to rule out the possibility completely. For a rigorous test of the given scenarios, higher cadence observations and more complete temperature coverage will be required.

5. Conclusions

Following the report by McKenzie & Hudson (1999) of supra-arcade downflows in an LDE flare, a data archive search was undertaken for similar events. In the period 01 January 1998 to 08 May 1999, 22 LDE arcades were found in the SXT data archive which possessed supra-arcade fans of the type described by Švestka et al. (1998) and McKenzie & Hudson (1999, Paper I). In 12 of these 22 events, supra-arcade downflows like those of Paper I were detected. Thus it was shown that the fraction of LDE arcades possessing fans is not small, and that downflows above such arcades are not uncommon. A comparison was drawn to the appearances of these arcade structures in SXR, in EUV, and in Hα where these latter two were available. Though the cadence of the available EUV and Hα sequences were not as fast as that of the SXR observations, it was felt that they had sufficient dynamic range and sensitivity to low levels of emission to enable detection of blobs of material above the flare arcades, if such blobs existed and had temperatures within the sensitivity bands of the given instruments. It was hoped that the combination of SXR, EUV, and Hα would give adequate sensitivity to emissions over a wide range of temperatures, though it is admitted that a significant gap in the temperature coverage exists.

This combinatory approach was designed in part to test the possibility that the X-ray voids reported in Paper I might be explained as evidence of blobs of relatively cool material separated from the main body of the CME and falling (gravitationally) back to the surface of the Sun. No direct evidence was found to support this interpretation.

The measured speeds of downflow are consistent with either gravitational freefall or magnetic field line shrinkage.

We therefore have no data which require adaptation of the standard explanation of the formation of coronal rain: the suggestion that CME material falls back to the post-flare loops to form coronal rain is not supported by these observations. Similarly the "above-the-arcade coronal rain" scenario of Paper I (scenario 1) is not supported.

However, the magnetic field line shrinkage scenarios proposed by Wang et al. (1999) and in Paper I (scenario 3) are not refuted. Although no shrinkage was directly observed in EUV, the soft X-ray sequences reveal a few cases of hot (i.e., X-ray emitting) material moving downwards, and some of these have looplike morphology. This tends to support the shrinkage explanation shared by Wang et al. and Paper I.

If the downward motions represent the dipolarization of reconnected field lines, then the location of the reconnection site must necessarily be high above the flare arcade, because the downflows are observed as high as 40 – 60 Mm above the top of the SXR arcade. Moreover the fact that these flows occur in the decay phase of the flares, sometimes for several hours beyond the SXR peak, would serve as direct indication that reconnection persists for a very long time after the initial eruption, consistent with the known fact that energy is released during the whole gradual phase of an LDE flare (Švestka 1989 and references therein). Most importantly, however, the observation of discrete downflowing features would indicate that the reconnection is not perfectly smooth and continuous, but proceeds piecewise. As demonstrated by Klimchuk (1997), such "patchy and intermittent" reconnection is to be expected in a true 3-dimensional modeling (rather than 2.5-D) of the magnetic field evolution in a post-eruption arcade. The entanglement and intertwining of magnetic field lines which must exist in an actual 3-D solar pre-eruption structure would seem to require that post-CME reconnection is not the orderly and smoothly organized process depicted in 2.5-D simulations. The present observations tend to support this: if they are to be interpreted as support for the standard Carmichael-Sturrock-Hirayama-Kopp-Pneuman reconnection scenario, then it must be admitted that 2.5-D modeling is not sufficient, but rather a truly 3-D model which includes patchy reconnection must be further developed.

Acknowledgements

The Hα data were provided by Mauna Loa Solar Observatory and the High Altitude Observatory. The EUV data were provided by the EIT Consortium, the Solar Data Analysis Center at NASA Goddard Space Flight Center, and the TRACE team. SOHO is a joint ESA-NASA program. TRACE is a NASA Small Explorer project. The *Yohkoh* Soft X-ray Telescope is a collaborative project of the Lockheed Palo Alto Research Laboratory, the National Astronomical Observatory of Japan, and the University of Tokyo, supported by NASA and ISAS. The author is grateful to Andrew Stanger for preparing the Hα data for analysis, to Hugh Hudson for helpful and encouraging discussions throughout the process of this study, to Jeff Newmark for providing a sanity check of the analysis of the EIT images, and to an anonymous referee for thoughtful and very helpful comments. This work was supported by

NASA under Marshall Space Flight Center contract NAS8-40801 with the Lockheed Martin Advanced Technology Center.

Appendix

A. Captions for Enclosures

Movies are included on the accompanying CD-ROM, in two formats: MPEG and JAVA Script. In each case, the MPEG movie (filename: *Enclosure_N.mpg*) will repeat four times; the JAVA Script movie (filename: *Enclosure_N.html*) is compatible with many web browsers.

A.1. Enclosure 1

Spanning the interval 06:55 – 07:12 UT of 23 April 1998, this movie shows downflow above the arcade in the form of X-ray voids. The upper arrow indicates the approximate location of some features which approach the top of the arcade near the end of the movie. The direction of motion of these particular features is distinctly non-radial; a heliographic coordinate grid is shown to emphasize the location of the solar limb. The speed of the motion in the north is approximately 370 km s^{-1} in the plane of the sky. Downward flows can also be detected other parts of the arcade, in particular above the position indicated by the lower arrow.

A.2. Enclosure 2

Spanning the interval 18:27 – 18:43 UT of 16 August 1998, this movie depicts one of the better examples of the apparent shrinkage of bright, X-ray emitting looplike features. These are especially visible near the arrow, but less distinct examples can be seen above the southern end of the arcade as well.

A.3. Enclosure 3

Spanning the interval 20:36 – 20:46 UT of 20 January 1999, this movie shows the downward directed flow field which was first discussed in Paper I. The arrows mark the positions of some of the more visible X-ray voids; speeds are between 90 – 500 km s^{-1} in the plane of the sky.

A.4. Enclosure 4

This color-reversed sequence shows the Hα images from Mauna Loa Solar Observatory during the same interval as the movie in Enclosure 3. Coronal rain is clearly evident, although Figure 3 demonstrates that the location of the Hα flow is far removed from the region in which the SXT downflows are observed. The bright two-ribbon flare at the footpoints of the arcade is clearly visible.

A.5. Enclosure 5

Spanning the interval 19:18 – 19:27 UT of 20 January 1999, this color-reversed movie depicts the brightening of the arcade during the rising phase of the M5.2 flare. A considerable amount of motion is visible above the entire length of the arcade, as well as the apparent retraction of a magnetic loop in the north end of the arcade: see Figure 2 and the discussion in section 3.10.

References

Cargill, P. J. & Priest, E. R. 1983, ApJ, 266, 383.
Delaboudiniere, J.-P., et al. 1995, Sol. Phys., 162, 291.
Foley, C., Culhane, J. L., & Acton, L. W. 1997, ApJ, 491, 933.
Forbes, T. G. & Acton, L. W. 1996, ApJ, 459, 330.
Forbes, T. G. & Malherbe, J. M. 1986, ApJ, 302 L67.
Foukal, P. V. 1976, ApJ, 210, 575.
Goldsmith, D. W. 1971, Sol. Phys., 19, 86.
Handy, B. N., et al. 1999, Sol. Phys., 187, 229.
Hiei, E., & Hundhausen, A. J. 1996, in Magnetodynamic Phenomena in the Solar Atmosphere, ed. Y. Uchida, T. Kosugi, & H. Hudson (Dordrecht: Kluwer), 125.
Klimchuk, J. 1997, in ASP Conf. Ser. 111: Magnetic Reconnection in the Solar Atmosphere, ed. R. D. Bentley & J. T. Mariska, 319.
McKenzie, D. E. & Hudson, H. S. 1999, ApJ, 519, L93.
Moses, D., et al. 1997, Sol. Phys., 175, 571.
Nitta, N. & Akiyama, S. 1999, ApJ, 525, L57.
Ohyama & Shibata 1997, PASJ, 49, 249.
Ohyama & Shibata 1998, ApJ, 499, 934.
Schmieder, B., Forbes, T. G., Malherbe, J. M., & Machado, M. E. 1987, ApJ, 317, 956.
Schrijver, C. J., et al. 1999, Sol. Phys., 187, 261.
Švestka, Z. 1987, Sol. Phys., 108, 237.
Švestka, Z. 1989, Sol. Phys., 121, 399.
Švestka, Z., Fárník, F., Hudson, H., & Hick, P. 1998, Sol. Phys., 182, 179.
Tsuneta et al. 1991, Sol. Phys., 136, 37.
Wang, Y.-M., Sheeley, N. R., Jr., Howard, R. A., St. Cyr, O. C., & Simnett, G. M. 1999, GRL, 26, 1203.